Static multi-crack modeling in concrete by a modified DR method

R. C. Yu & G. Ruiz
ETSI Caminos, C. y P., Universidad de Castilla-La Mancha, Ciudad Real, Spain

ABSTRACT We aim to model static multi-cracking processes in concrete. The explicit dynamic relaxation (DR) method, which gives the solutions of non-linear static problems on the basis of the steady-state conditions of a critically damped explicit transient solution, is chosen to deal with the present high geometric and material non-linearities. One of the common difficulties of DR method is its slow convergence rate when non-monotonic spectral response is involved. A modified concept that is distinct from the standard DR method is introduced to tackle this problem. The methodology is validated against the three point bending test on notched concrete beams of different size, the solutions along the whole load-displacement curve, specially the peak load, the post-peak behavior follow closely after the experiments results; the size effect is caught naturally as a result of the calculation, micro cracking and non-uniform crack propagation across the fracture surface also come out directly from the 3D simulations.

Keywords: dynamic relaxation, cohesive elements, self adaptive remeshing.

1. INTRODUCTION

We aim to model static multi-cracking processes in a quasi-brittle materials like concrete. In the literature, the viability of cohesive theories of fracture applied to the dynamic regime has been demonstrated by Ortiz and his coworkers (Camacho 1996, Pandolfi 1999, Ruiz 2000, Ruiz 2001). Multi-cracking processes were modeled by inserting cohesive surfaces between the elements defining the original mesh. The crack propagation was led by a fragmentation algorithm that was able to modify the topology of the mesh at each iteration. However, the modeling of crack propagation within static regime has been hindered by the difficulties to find efficient and stable numerical algorithms which are able to deal with high geometric and material nonlinearities.

One feasible way to solve non-linear static problems is based on the steady-state conditions of a critically damped transient solution, often termed as dynamic relaxation (DR). In searching the solution, the DR method sets an artificial dynamic system of equations, with added fictitious inertia and damping terms, and lets it "*relax*" itself to the real solution of the physical problem. This simple and effective way of dealing non-linear problems has been used for some time in general structural applications (Otter 1965, Brew 1971, Pica 1980, Papadrakakis 1981, Sauve 1995), in rolling (Chen 1989), bending with wrinkling (Zhang 1989) as well as creep (Sauvé 1993), since Day first introduced the method in 1960s (Day 1965). Siddiquee (Siddiquee 1995) also used DR to trace the equilibrium path in materially non-linear problems. Essentially, the DR method is used to maintain the advantages of an explicit method compared to an otherwise implicit approach. In principle, if the physical problem has a solution, it will be reached *sooner or later*, then the difficulties are passed on to efficiently enhance the relaxation process.

Besides the use of parallel computing, different aspects in the effectiveness of DR have been

investigated by a series of authors, including the adaptive adjustment of the loading rate (Rericha 1986), the use of adaptive damping (Sauvé 1996), and the effectiveness of constraints and mesh transitions on the convergence rate (Metzger 1997). Along the time, a general procedure for DR has been formulated to solve a wide range of problems, this includes a lumped mass matrix, a mass proportional damping matrix and a standard way called Rayleigh's quotient to estimate the damping coefficient based on the participating frequency of the structural response. Following this line, Oakley and Knight (Oakley 1995a,b,c) have given detailed implementations for single processors as well as parallel processor computers. However, the performance of DR is highly dependent on the properties of the problem (Metzger 2003).

In particular, our model to study cpmplex fracture processes in concrete is very non-linear. This non-linearity stems both from the cohesive laws governing the opening of the crack and the from the constant insertion of new elements. The standard estimation of the critical damping coefficient is done through Rayleigh's coefficient, which damps the system from higher frequency mode to lower frequency mode. When there is cracking, the estimation gives a higher frequency mode, which actually stalls the motion and makes the convergence rate unacceptably slow. We have found out that by damping the system in two successive steps through two criteria, the calculations could be greatly enhanced. During the first stage, after loading, with the added inertia and damping terms, the system is artificially set in motion, and this motion is necessarily to be kept as strong as possible in order to be felt by the whole system; this can only be realized through "under-damping", i.e., adopting a damping coefficient smaller than the one given by the Rayleigh estimation. Once the motion has reached the whole system, in the second step, the critical damping is adopted so that the system could reach its steady state in the fastest possible rate. By so doing, the convergence of solution could be increased by a magnitude of ten or more; therefore makes the solution procedure acceptable to the scale of the problem considered.

The organization of the paper is as the following. Next comes a brief review of the cohesive model. The formulation of the explicit dynamic relaxation method is presented afterwards and the simulation results as well as the comparisons with the experiments are discussed at the end.

2. THE COHESIVE MODEL

For completeness, we summarize here the main features of the cohesive model used in the calculations. A complete account of the theory and its finite-element implementation may be found elsewhere (Camacho 1996b, Ortiz 1999). A variety of mixed-mode cohesive laws accounting for tension-shear coupling, is obtained by the introduction of an effective opening displacement δ, which assigns different weights to the normal δ_n and sliding δ_s opening displacements.

$$\delta = \sqrt{\beta^2 \delta_s^2 + \delta_n^2} \tag{1}$$

Assuming that the cohesive free-energy density depends on the opening displacements only through the effective opening displacement δ, a reduced cohesive law, which relates δ to an effective cohesive traction t.

$$t = \sqrt{\beta^{-2} t_s^2 + t_n^2} \tag{2}$$

where t_s and t_n being the amplitude of the shear and the normal tractions, respectively, can be obtained (Camacho 1996b, Ortiz 1999). The weighting coefficient β defines the ratio between the shear and the normal critical tractions. We assume the existence of a loading envelope defining a relation between t and δ under the conditions of monotonic loading and irreversible unloading. A simple and convenient type of irreversible cohesive law, typical of concrete and recommended by the Model Code, is furnished by the bi-linearly decreasing envelope, characterized by Equation 3.

$$
\begin{aligned}
t &= \sigma_c (1 - 0.85\,\delta/\delta_c) \\
&\qquad 0 < \delta < \delta_a \\
t &= 0.15\,\sigma_c (\delta_c - \delta)/(\delta_c - \delta_a) \\
&\qquad \delta_a < \delta < \delta_c \\
t &= 0 \\
&\qquad \delta \geq \delta_c
\end{aligned}
\tag{3}
$$

where δ_a and δ_c are determined through the following equations

$$
\begin{aligned}
\delta_a &= (2 - 0.15\,\beta_F) G_F / f_{ts} \\
\delta_c &= \beta_F G_F / f_{ts}
\end{aligned}
\tag{4}
$$

In which, f_{ts} is the static tensile strength, G_c is the material fracture energy, β_F is related to the maximum aggregate size d_m, for the case of d_m = 5 mm, β_F can be taken roughly to be 8.4 (Ruiz 1998), which is used in the simulations later on.

Cohesive theories introduce a well-defined length scale into the material description and, in consequence, are sensitive to the size of the specimen (see, for example, Planas 1998). The characteristic length of the material may be expressed as

$$
l_{ch} = E G_c / f_{ts}^2 \tag{5}
$$

where E is the material elastic modulus.

In the calculation, only decohesion along element boundaries is allowed to occur. When the critical cohesive traction is attained at the interface between two volume elements, a cohesive element is inserted at that location using a fragmentation algorithm (Pandolfi 2002). This cohesive element governs the opening of the cohesive surface.

3. THE EXPLICIT DYNAMIC RELAXATION METHOD

As we mentioned before, in calculations, the fracture surface is confined to inter-element boundaries and, consequently, the structural cracks predicted by the analysis are necessarily rough. Even though this numerical roughness in concrete can be made to correspond to the physical roughness by simply choosing the element size to resolve the cohesive zone size (Ruiz 2001), the nonlinearity of the solution thus induced plus the material nonlinearity is difficult to handle in static regime for traditional solvers. We choose explicit dynamic relaxation method as an alternative to tackle this situation, the standard formulation of this methodology is summarized below.

Consider the system equations for a static problem at a certain load step n

$$
\boldsymbol{F}^i (\boldsymbol{u}_n) = \boldsymbol{F}^e_n \tag{6}
$$

where $\boldsymbol{u}_n$ is the solution array (displacements), $\boldsymbol{F}^i$ and $\boldsymbol{F}^e_n$ are the internal and external force vectors. Following the ideas of dynamic relaxation, Equation 6 is transformed to a dynamic system by adding both artificial inertia and damping terms.

$$
\boldsymbol{M}\,\boldsymbol{a}_n + \boldsymbol{C}\,\boldsymbol{v}_n + \boldsymbol{F}^i(\boldsymbol{u}_n) = \boldsymbol{F}^e_n \tag{7}
$$

where $\boldsymbol{M}$ and $\boldsymbol{C}$ are the fictitious mass and damping matrices, $\boldsymbol{a}_n$ and $\boldsymbol{v}_n$ are acceleration and velocity vectors respectively at load step n. The solution of Equation (7) can be obtained by the explicit time integration method using the standard central difference integration scheme in two steps.

First the displacements and predictor velocities are obtained

$$
\begin{aligned}
\boldsymbol{u}_n^{t+1} &= \boldsymbol{u}_n^t + dt\,\boldsymbol{v}_n^t + dt^2\,\boldsymbol{a}_n^t/2 \\
\boldsymbol{v}_{npred}^{t+1} &= \boldsymbol{v}_n^t + dt\,\boldsymbol{a}_n^t/2
\end{aligned}
\tag{8}
$$

Second the internal force vector is updated and the accelerations and corrected velocities are obtained.

$$
\begin{aligned}
\boldsymbol{a}_n^{t+1} &= (\boldsymbol{M} + dt\,\boldsymbol{C}/2)^{-1} \\
&[\boldsymbol{F}^e_n - \boldsymbol{F}^i(\boldsymbol{u}_n^{t+1}) - \boldsymbol{C}\,\boldsymbol{v}_{npred}^{t+1}] \\
\boldsymbol{v}_n^{t+1} &= \boldsymbol{v}_{npred}^{t+1} + dt\,\boldsymbol{a}_n^{t+1}/2
\end{aligned}
\tag{9}
$$

Both fictitious mass $\boldsymbol{M}$ and damping $\boldsymbol{C}$ matrices are set to be diagonal to preserve the explicit form of the time-stepping integrator. At the same time,

the damping matrix is set to be proportional to the mass matrix through the damping coefficient ξ.

$$\boldsymbol{C} = \xi \boldsymbol{M} \tag{10}$$

To ensure that the mode associated with the applied loading condition is critically damped, ξ is generally set to be

$$\xi = 2\omega \tag{11}$$

where ω is the undamped natural frequency corresponding to the participating mode of loading.

Since both the inertia and damping terms are artificial, the dynamic relaxation parameters, including the mass matrix $\boldsymbol{M}$, the damping coefficient ξ and time step dt, can be selected to produce faster and more stable convergence to the static solution of the real physical system.

Owing to the explicit formulation, the time step must satisfy the stability condition

$$dt \le h_m / c_d \tag{12}$$

where h_m is the size of the smallest element, c_d is the speed of a dilatational wave, which in turn, can be related to ω_m, the highest undamped frequency of the discretized system through

$$\omega_m = 2 c_d / h_m \tag{13}$$

For an elastic material, the dilatational wave speed is calculated as

$$c_d = \sqrt{(\lambda + 2\mu)/\rho} \tag{14}$$

where λ and μ are Lamé constants, while ρ is the material density.

Equations 12, 13 and 14 provide a relation between the maximum admissible time step, $dt_{cr} = 2/\omega_m$ and the fictitious mass matrix.

$$\rho \ge (\lambda + 2\mu)[\, dt_{cr} / h_m \,]^2 \tag{15}$$

In the implementation, the density is adjusted for each element so that the time for the elastic wave to travel through every element is the same.

The current value of ω is estimated at each iteration t using Rayleigh quotient

$$\omega^t = \sqrt{(\boldsymbol{u}^t)^T \boldsymbol{K}\, \boldsymbol{u}^t / (\boldsymbol{u}^t)^T \boldsymbol{M}\, \boldsymbol{u}^t} \tag{16}$$

where $\boldsymbol{u}^t$ stands for the displacement vector at the t^{th} iteration (index n has been ommitted) and $\boldsymbol{M}$ is the mass matrix. For nonlinear problems, $\boldsymbol{K}$ represents a diagonal estimate of the tangent stiffness matrix at the t^{th} iteration and is given by

$$\boldsymbol{K}^t = \frac{\boldsymbol{F}^i(\boldsymbol{u}^t) - \boldsymbol{F}^i(\boldsymbol{u}^{t-1})}{\boldsymbol{u}^t - \boldsymbol{u}^{t-1}} \tag{17}$$

4. THE MODIFIED DR METHOD

As we mentioned before, one of the common difficulties of DR method is its slow convergence rate when non-monotonic spectral response is involved. The standard estimation of the critical damping coefficient is through Rayleigh's coefficient, which damps the system from higher frequency mode to lower frequency mode. During the calculations for non-linear problems, when the estimation gives a higher frequency mode, the damping coefficient adopted will overdamp the global motion and actually stalls the system and makes the convergence rate unacceptably slow. In dealing with this difficulty, instead of critically damping the system equations from the beginning as suggested by all the standard DR procedures, we intend to keep the motion as strong as possible, so that the local movement excited at the loading area could be fastly spreaded to the rest; this can only be done through ``under-damping'', i.e., adopt a damping coefficient smaller than the one estimated by the current Rayleigh estimation. Simply no-damping or low damping may keep a noisy response persist. We found out that by setting the damping coefficient close to half of the undamaged system (which was obtained through the Rayleigh quotient estimation in the trial run),

the motion can be kept strong so that the system could move faster toward its external force equilibrium without carrying persisting noisy response. Once the external force equilibrium is achieved, in the next stage, the system is critically damped to its steady state to obtain the static solution. Taking into account the aforementioned considerations, we implement two combined convergence criteria to be used successively during the two steps of the iteration process. One is the ratio between the sum of external imposed forces and reaction forces and the estimated maximum external forces, the measure that says to what extent the motion has spreaded to the whole system; the other is the relative global kinetic energy, which measures whether the system is approaching static or not. This combined criteria is characterized by the following inequalities

$$\frac{\|F_{rt}+F_{ip}\|_2}{\|F_e\|_2} < f_{tol}$$
$$\frac{\sum m\,(v^t)^2 \;/2}{K_0} < ke_{tol} \qquad (18)$$

where $\|\ \|_2$ denotes the Euclidean norm, $\boldsymbol{F}_{rt}$ are the reaction forces at the supports, $\boldsymbol{F}_{ip}$ are the imposed forces at the loading point; m is the nodal mass; K_0 is a constant used to normalize the kinetic energy, whose value varies according to the size of the problem and is chosen to avoid unproductive iteration cycles. The tolerances f_{tol} and ke_{tol} are taken as 0.001 and 10^{-8} respectively. For the problems we have considered, these tolerances provide a good balance of accuracy and efficiency. A damping coefficient ξ_0 is computed after the first insertion of the cohesive element takes place, or when the nonlinearity of the material started to emerge. By setting the damping coefficient to this value when the solution is far away from the equilibrium, while using the critical damping coefficient computed when the solution is near static, the global convergence rate is remarkably enhanced.

5. NUMERICAL APPLICATIONS -- THREE POINT BENDING NOTCHED BEAMS

We apply the modified dynamic relaxation method to solve the static propagation of a crack through a notched concrete beam subjected to three point bending, see Figure 1.

In previous studies, Camacho and Ortiz (Camacho 1996) have noted that the accurate description of fracture processes by means of cohesive elements requires the resolution of the characteristic cohesive length of the material. Further studies (Ruiz 2001) showed that in concrete, the element size can be made to be comparable to the maximum aggregate size, which is 5 mm in our case. So all specimens are discretized into ten-node quadratic tetrahedral elements and have element size of 6 mm near the middle surface. The material parameters for the concrete given in Table 1 are taken from the experiments of Ruiz (Ruiz 1998).

Table 1. Concrete mechanical properties

f_{ts} (MPa)	E(GPa)	G_c(N/m)	l_{ch}(mm)
3.8	30.5	62.5	130.

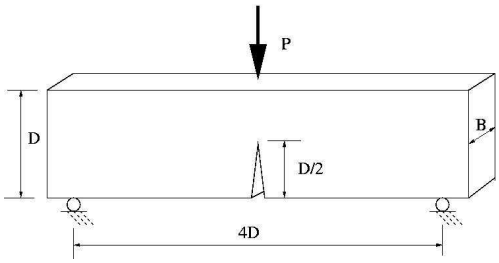

Figure 1. The notched concrete beam subjected to three point bending, where B=50 mm, D=75, 150 or 300 mm.

5.1 Initial damping coefficient

In this section, we choose one loading step within the calculation for the small specimen to show the improved convergence rate using the modified DR method. During the loading processes, in searching the solution, we divide the process into two, first the specimen is loaded with a small increase of

displacements; then the program checks the traction of all the element interfaces, if the opening criterion is satisfied, a cohesive element would be inserted there, and consequently, before moving to the next load increment, an iteration loop would be carried out to adjust the solutions because of the stress release coming from the crack propagation.

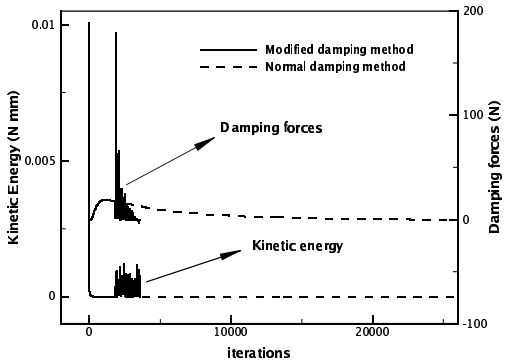

Figure 2. Damping forces and kinetic energy comparisons for the normal and modified damping procedures in the case of the specimen a.

In Figure 2, we compare the modified dynamic relaxation procedure with the standard one for the small specimen at loading displacement 0.0224 mm, during which two new cohesive elements were inserted. The figure depicts the evolution of damping forces and kinetic energies according to the iteration number. Since the dynamic equilibrium has been enhanced by previous iterations during the loading step, the two methods give the same damping forces and kinetic energy until at some point, the system realize that it is going away from its equilibrium. The standard dynamic relaxation tries to critically damp the system all the time, even though the damping force is decreasing dramatically and the kinetic energy goes to almost zero, the motion is actually stalled. Whereas the modified dynamic relaxation, when it is away from its equilibrium, instead of critically damping the fast motion, it under-damps the high frequency motion, so instead of being damped, the system actually *regains* its movement, therefore moves faster to its equilibrium state; once the force equilibrium is achieved, the critical damping is adopted to bring the kinetic energy quickly to zero.

In the example shown, where the nonlinearity is not so strong, for the standard DR method, it takes the 25785 iterations, while for the modified DR method, only 3625 iterations are needed for the same convergence criteria adopted. This means a gain of more than 7 times regarding to the rate convergence. While in the situation of higher non-linearity (the post-peak), the comparison is not possible, simply because the normal DR method would take unacceptable time to the arrive the solution of the static system.

5.2 The load-displacement curve comparison

The modified concept is applied to three specimens of different size. The cohesive law adopted in the calculation is the one suggested in the Model Code for concrete, Equation 3. The load versus displacement curves for all specimens, compared with the experimental results, are shown in Figure 3. The calculated maximum load only differs 0.4% from the experimental one for the small specimen, 3.0% for the intermediate one and 10.0% for the large specimen. The experimentally observed size effect comes naturally from the simulations.

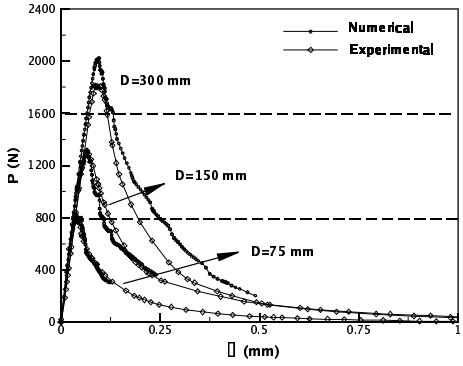

Figure 3. The peak load comparison for three specimens of depth 75, 150 and 300 mm.

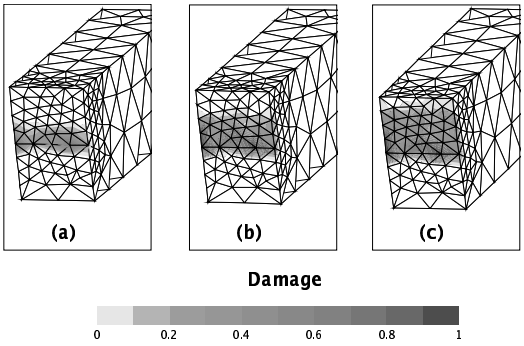

Figure 4. Sanp shots of the fracture patterns (at the middle surface for the small specimen with depth 75mm) developed loading displacement (1) 0.05 mm (b) 0.07 mm (c) 0.11 mm.

5.3 Fracture patterns

Three snapshots of the fracture patterns on mid-plane for the small specimen are shown in Figure 4, where the displacements have been magnified 100 times to aid visualization. Figure 4a is the point of peak load, Figure 4c is the moment where the beam is almost completely crushed, while Figure 4b is a point in between which shows how the fracture zone has developed. Also shown in the figures are the level contours of damage, defined as the fraction of expended fracture energy to total fracture energy per unit surface, or critical energy release rate. Thus, a damage density of zero denotes an uncracked surface, whereas a damage density of one is indicative of a fully cracked or free surface. The transition zone wherein the damage variable takes intermediate values may be regarded as the cohesive zone, and the crack front may conventionally be identified with the level contour of 1/2. It can be noticed that in the peak load, Figure 4a, the fracture zone has developed to some degree, only that the crack surfaces are not fully open yet; later on in Figure 4b, the same zone is more developed while new surfaces are open and the crack front propagates in a nonuniform way, which can only be observed in a full three-dimensional modeling. It is interesting to note that the crack front is convex in the direction of propagation, a feature which is characteristic of mode-I crack growth, the exterior of the crack front ostensibly lags behind the interior points. In Figure 4c, the crack continues to grow till the specimen is almost completely crushed and loses its strength.

6. SUMMARY AND CONCLUSIONS

We have put together an modified explicit dynamic relaxation method in conjunction with the cohesive theory to solve the static multi-cracking fracture process notched concrete beams loaded at three points. In calculations, the fracture surface is confined to inter-element boundary elements and, consequently, the structural cracks predicted by the analysis are necessarily rough. Even though this numerical roughness in concrete can be made to correspond to the physical roughness by choosing the element size comparable to the aggregate size, the thus-induced geometrical nonlinearity and the material nonlinearity inherent to concrete are hard to handle for traditional static solvers. The explicit DR method is chosen as an alternative, to approach this problem. We have followed the ideas of Underwood (Underwood 1983) and Oakley (Oakley 1995b) for fictitious mass and damping matrices but implemented the method with a concept that is distinct from the standard one. An initial damping coefficient estimated from the system is adopted to *enhance* the motion instead of critically damping it from the beginning. A criterion that measures the force balance is used to control the iterations in this stage; while the global kinetic energy is chosen to control the balance of accuracy and efficiency of the solution for the static system. Three sizes of concrete beams with different depth were modeled to validate against the experimental results of Ruiz (Ruiz 1998). The results show that the model captures the peak load accurately, the load-displacement curve follows closely the experimental results before and after the peak load. A comparison of convergence rate between the standard and modified DR method reveals the modified concept eliminates the stalling part of the traditional DR method and makes it a feasible and efficient solution technique for the problem considered.

7. ACKNOWLEDGMENTS

R.C. Yu thanks the *Ministerio de Ciencia y Tecnología (MCYT)*, Spain, for the financail support for her research given under the *Ramón y Cajal* Program. G. Ruiz acknowledges financial support from the *MCYT*, Spain, under grants MAT2000-0705 and MAT2003-0843.

8. REFERENCES

Bažant, Z.P. & Planas, J. 1998. *Fracture and Size Effect in Concrete and Other Quasibrittle Materials*. CRC Press, Boca Raton, Florida.

Brew, J.S. & Brotton, D.M. 1971. Non-linear structural analysis by dynamic relaxation. I*nternational Journal for Numerical Methods in Engineering*,3: 436--483.

Camacho, G.T. & Ortiz, M 1996. Computational modeling of impact damage in brittle materials. *International Journal of Solids and Structures*,33(20-22):2899—2938.

Chen,B.K. & Choi, S.K. & Thomson, P. F. 1989. Analysis of plane strain rolling by the dynamic relaxation method. I*nternational Journal of Mechanical Sciences,* 31(11/12):839—851.

Day, A.S 1965. An introduction to dynamic relaxation. *The Engineer*, 219:218—221

Metzger, D.R. & Sauvé, R.G. 1997. The effect of discretization and boundary conditions on the convergence rate of the dynamic relaxation method. Current Topics in the Design and Analysis of Pressure Vessels and Piping, *ASME PVP*, 354:105—110.

Metzger, D.R. 2003. Adaptive damping for dynamic relaxation problems with non-monotonic spectral response. International Journal for Numerical Methods in Engineering, 56:57--80.

Oakley, D.R. & Knight., N.F.Jr. 1995a. Adaptive dynamic relaxation algorithm for non-linear hyperelastic structures. part i. Formulation. *Computer Methods in Applied Mechanics and Engineering*,126:67--89.

Oakley, D.R. & Knight., N.F.Jr. 1995b. Adaptive dynamic relaxation algorithm for non-linear hyperelastic structures. part ii. single processor implementation. *Computer Methods in Applied Mechanics and Engineering*,126:91--109.

Oakley, D.R. & Knight., N.F.Jr. 1995c. Adaptive dynamic relaxation algorithm for non-linear hyperelastic structures. part iii. parallel implementation. *Computer Methods in Applied Mechanics and Engineering*,126:111--129.

Ortiz, M. & Pandolfi, A. 1999. Finite-deformation irreversible cohesive elements for three-dimensional crack-propagation analysis. *International Journal for Numerical Methods in Engineering*, 44:1267—1282.

Otter, J.R.H. 1965. Computations for prestressed concrete reactor pressure vessels using dynamic relaxation. *Nucl. Struct. Engng*.1: 61—75.

Pandolfi, A. & Krysl,P. & Ortiz,M. 1999. Finite element simulation of ring expansion and fragmentation. I*nternational Journal of Fracture*, 95:279—297.

Pandolfi, A. & Ortiz, M. 2002. An efficient adaptive procedure for three-dimensional fragmentation simulations. *Engineering with computers*, 18(2):148—159.

Papadrakakis, M. 1981. A method for automated evaluation of the dynamic relaxation parameters. *Computer Methods in Applied Mechanics and Engineering*,25:35—48.

Pica,A. & Hinton, E.1980 Transient and pseudo-transient analysis of mindlin plates. *International Journal for Numerical Methods in Engineering*,15:189—208.

Rericha, P. 1986. Optimum load time history for non-linear analysis using dynamic relaxation. *International Journal for Numerical Methods in Engineering,* 23:2313--2324.

Ruiz, G. & Ortiz,M. & Pandolfi, A. 2000. Three-dimensional finite-element simulation of the dynamic Brazilian tests on concrete cylinders. *International Journal for Numerical Methods in Engineering*, 48: 963--994.

Ruiz, G. & Ortiz,M. & Pandolfi, A. 2001. Three-dimensional cohesive modeling of dynamic mixed-mode fracture. I*nternational Journal for Numerical Methods in Engineering,* 52: 97--120.

Ruiz, G. 1998. Influencia del Tamaño y de la Adherencia en la Armadura mínima de Vigas en Flexión. *Grupo Español del Hormigón*, Madrid, Spain.

Sauvé, R.G. & Badie, N. 1993. Nonlinear shell formulation for reactor fuel channel creep. In Design Analysis , Robust Methods and Stress Classification,Bess WJ(ed.), *ASME PVP*, 265:269--275.

Sauvé, R.G. & Metzger, D.R. 1995. Advances in dynamic relaxation techniques for nonlinear finite element analysis.*Transactions of the ASME*, 117:170--176.

Sauvé, R.G. & Metzger, D.R. 1996. A hybrid explicit solution technique for quasi-static transients. In Computer Technology Applications and Methodology, Hulbert GM(ed.),*ASME PVP*, 326:151—157.

Siddiquee,MSA & Tanaka,T. & Tatsouka F. 1995.Tracing the equilibrium path by dynamic relaxation in materially nonlinear finite element problems. *International Journal for Numerical and Analytical Methods in Geomechanics*, 19:749--767.

Underwood, P.G, 1983. Dyanmic relaxation. *Computational Methods for Transient Analysis,* (1):145—265,

Zhang, L.G. & Yu, T.X. 1989. Modified adaptive dynamic relaxation method and its application to elastic-plastic bending and wrinkling of circular plates. Computers and Structures, 33(2) 839—851.